Vision Research 100 (2014) 56–71

Contents lists available at ScienceDirect

Vision Research

journal homepage: www.elsevier.com/locate/visres

Cortical responses to optic flow and motion contrast across patterns and speeds

Jeremy D. Fesi [a,*], Amanda L. Thomas [b], Rick O. Gilmore [b,c]

[a] Department of Ophthalmology, McGill University, 687 Pine Avenue West, Montreal, QC H3A 1A1, Canada
[b] Department of Psychology, The Pennsylvania State University, 114 Moore Building, University Park, PA 16802, United States
[c] Social, Life, & Engineering Sciences Imaging Center, The Pennsylvania State University, University Park, PA 16802, United States

ARTICLE INFO

Article history:
Received 19 February 2013
Received in revised form 5 March 2014
Available online 19 April 2014

Keywords:
Motion
Optic flow
Motion contrast
SSVEP
Electrophysiology

ABSTRACT

Motion provides animals with fast and robust cues for navigation and object detection. In the first case, stereotyped patterns of optic flow inform a moving observer about the direction and speed of its own movement. In the case of object detection, regional differences in motion allow for the segmentation of figures from their background, even in the absence of color or shading cues. Previous research has investigated human electrophysiological responses to global motion across speeds, but only focused upon one type of optic flow pattern. Here, we compared steady-state visual evoked potential (SSVEP) responses across patterns and speeds, both for optic flow and for motion-defined figure patterns, to assess the extent to which the processes are pattern-general or pattern-specific. For optic flow, pattern and speed effects on response amplitudes varied substantially across channels, suggesting pattern-specific processing at slow speeds and pattern-general activity at fast speeds. Responses for coherence- and direction-defined figures were comparatively more uniform, with similar response profiles and spatial distributions. Self- and object-motion patterns activate some of the same circuits, but these data suggest differential sensitivity: not only across the two classes of motion, but also across the patterns within each class, and across speeds. Thus, the results demonstrate that cortical processing of global motion is complex and activates a distributed network.

1. Introduction

Motion provides important information about self-movement as well as for the detection of objects. In the first case, the surroundings of a mobile observer move past the observer's visual field in stereotyped patterns of motion known as optic flow. These patterns provide information about the direction and speed of the observer's movement through stationary surroundings (Gibson, 1950; Warren & Hannon, 1988). The dominant pattern of optic flow is radial expansion, associated with forward translation in depth (De Jong et al., 1994). Additionally, movements of the eyes and head contribute patterns of rotation and linear translation to the optic flow field (Britten, 2008). In the case of object detection, regional differences of motion known as motion contrast (Regan & Beverley, 1984) due to either observer or object motion allow for the segmentation of a figure from its background. This segmentation typically occurs via differences in the speed or direction of a figure relative to its surroundings. Segmentation by speed may reflect motion parallax – a cue to relative depth order (Rogers & Graham, 1979) where an object's retinal speed is inversely related to its distance from the observer (Ono, Rivest, & Ono, 1986; Rivest, Ono, & Saida, 1989) – object motion, or both. There is also a direction contrast that results from motion parallax, where objects closer than the point of fixation appear to move opposite the observer's direction of motion, while objects beyond the point of fixation appear to move in the same direction as the observer. Beyond this exception, however, direction contrast reflects object motion that goes against the global flow pattern associated with an observer's movement, and thus provides a cue that there is an object moving relative to the background.

Optic flow and motion contrast have often been studied separately, and yet they share important commonalities. For instance, when a predator pursues its prey, it must follow the movements of the prey "object" while also navigating its own body through complex or varied terrains. The interaction of form and motion cues in the brain is therefore important for the study of natural behaviors, yet the extent to which the processing of self- and object-related motion information overlap in the brain is not well

* Corresponding author. Address: McGill Vision Research, Department of Ophthalmology, 687 Pine Avenue West, Rm. H4-14, Montreal, QC H3A 1A1, Canada.
E-mail address: jeremy.fesi@mail.mcgill.ca (J.D. Fesi).

http://dx.doi.org/10.1016/j.visres.2014.04.004
0042-6989/

understood. One basic commonality between optic flow and motion contrast is that both depend upon the aggregation of local motion signals in the brain, either for global integration or regional segmentation (Berzhanskaya, Grossberg, & Mingolla, 2007; Marr & Hildreth, 1980). Among primates, motion direction selective cells are first detected in primary visual cortex (V1) (Hubel & Wiesel, 1968), while higher regions of visual cortex show sensitivity to motion patterns across larger regions of visual field. Neurophysiological studies on monkeys and humans suggest that the middle temporal (MT) area of macaques (V5 or hMT in humans) is crucial for motion integration (Born & Bradley, 2005; Britten et al., 1992; Newsome & Pare, 1988), as well as regional segmentation (Born & Tootell, 1992; Born et al., 2000; Likova & Tyler, 2008; Marcar et al., 1995; Pack, Gartland, & Born, 2004). Recent fMRI evidence has shown that different types of global motion patterns activate a network of areas including V6 (Cardin & Smith, 2010; Cardin et al., 2012), human MST (Cardin et al., 2012), and the posterior cingulate (Fischer et al., 2012).

Developmental evidence suggests that the mature motion processing network emerges over a prolonged developmental period. Infants and adults show similar steady-state visual evoked potential (SSVEPs) response profiles to local motion, but differ in their response to rotational flow patterns with temporally modulating motion coherence (Hou et al., 2009). Infants' SSVEP responses peak at large displacements/fast speeds, whereas adults' peak at small displacements/slow speeds. Behavioral evidence from both monkey (Kiorpes & Movshon, 2004) and human children (Hadad, Maurer, & Lewis, 2010) supports the claim that speed sensitivity shifts from fast to slow across primate visual development. Further, sensitivity to different patterns of optic flow may develop at different rates. Infants show larger SSVEPs to direction-reversing linear flows, while adults show the largest responses to radial flows (Gilmore et al., 2007). Thus, whether adults show responses to optic flow that differ by speed and pattern is an important unanswered question. By the same token, do object-related motion contrast responses show speed or pattern tuning? There is limited developmental evidence, but Fesi et al. (2011) found similar SSVEP response curves to different types or patterns of motion contrast among adults, keeping speeds constant. Thus, we do not know whether motion contrast responses vary with speed. Comparing optic flow and motion contrast responses may shed light on the extent to which cortical mechanisms for the processing of these two types of complex motion are distinct. The data may also provide benchmarks for future studies of the development of the primate motion processing network.

In the current experiments, we assessed in adults the effects of pattern and speed on SSVEP response sensitivity, first across optic flow patterns, and then across motion contrast types.

2. Experiment 1: optic flow

2.1. Method

2.1.1. Participants

Two groups of 20 adults (10 female in each group; mean age: 21.15 years) participated in this experiment. Subjects were recruited from an undergraduate subject pool for research credit, or were research assistants who volunteered to participate. All subjects had normal or corrected-to-normal vision, as determined by a brief evaluation of binocular Snellen optotype acuity.

2.1.2. Display

Subjects viewed random dot kinematogram displays on a monochrome monitor with an 800×600 pixel resolution and a screen refresh rate of 72 Hz. The displays were generated on a Macintosh G4 computer using Power Diva software (version 3.4, Smith-Kettlewell Eye Research Institute). Subjects viewed 2659 white dots (7 arcmin; luminance 72 cd/m^2) moving against a black background (0.6 cd/m^2). At the viewing distance of 60 cm, the display subtended $24^\circ \times 24^\circ$ visual angle. Dot positions were updated at 24 Hz.

Fig. 1 shows a schematic depiction of the displays used in the experiment. Displays featured dot motion modulating from 100% coherent global motion (indicating dot motion along a mean direction with a range of 0°) to 0% coherent motion (indicating dot motion along the same mean direction, but with a direction range of 360° for each dot) at a fixed temporal frequency of 1.2 Hz, referred to as the fundamental frequency, or F1. A full 100% coherent/incoherent display cycle took 833 ms.

All subjects viewed three optic flow pattern types (radial, rotation, and left/right linear translation) at three different speed settings. Thus, each subject viewed a total of nine conditions, with ten trials recorded per condition (yielding a total of 90 trials per subject session). Separate groups of participants viewed one of two ranges of dot speed settings. Speed Group 1 viewed displays with 5, 10, and 20 arcmin displacements per dot update. At the dot update rate of 24 Hz, this yielded dot speeds of 2, 4, and 8 deg/s, respectively. Speed Group 2 viewed displays with 2.5 arcmin/update (1 deg/s), 10 arcmin/update (4 deg/s), and 40 arcmin/update (16 deg/s) speeds.

Displays were presented within an annular area 24° in outer diameter and 4.77° in inner diameter. This was meant to reduce the effect of speed differentials that occur in the fovea of the rotation condition due to the constant linear (not rotational) speed constraint. The annular mask also reduced the luminance anisotropy associated with dot density variations in the radial condition when dots expand away from or contract toward the center. A small hole cut into the inner mask permitted participants to see a fixation cross.

2.1.3. Procedure

Participants were instructed to fixate on center of the fixation cross and to try not to move or blink during trials. Each trial consisted of ten 833 ms cycles, for a total duration of 8.33 s. Ten trials were recorded for each condition, and recording sessions typically lasted about 30 min. To minimize direction-selective adaptation, conditions were recorded in blocks, with each of the nine conditions being presented once per block, in random order. Participants were encouraged to rest or close their eyes between recording blocks. An experimenter remained in the recording chamber during recording to monitor the gaze of the participant throughout each trial to ensure that fixation was maintained. From this vantage point, the experimenter could detect eye position changes from fixation in the range of 3–5°.

2.1.4. VEP recording and analysis

Steady-state evoked potential (SSVEP) responses were recorded via a 128-electrode dense array (SensorNet, Electrical Geodesics, Inc.). The electrodes were referenced to the vertex (Cz), and then re-referenced to the net average. EEG was sampled at a rate of 443.52 Hz and low pass filtered at 50 Hz. Electrode impedance for each session was at or below 50 kOhms for all electrodes. Artifact rejection parameters were employed to reject display cycles containing raw amplitudes that exceeded a threshold of 50 μV, as well as entire trials with 15% of rejected cycles. Activity was analyzed offline via PowerDiva Host 3.4 software. The software analyzes EEG patterns using a version of the discrete Fourier transform. Responses that occurred at integer harmonics of the modulation frequency (1.2 Hz, F1) of the displays and the monitor (24 Hz, F2) and were phase-locked to the stimulus are reported here. Topographic visualizations of the data were created with

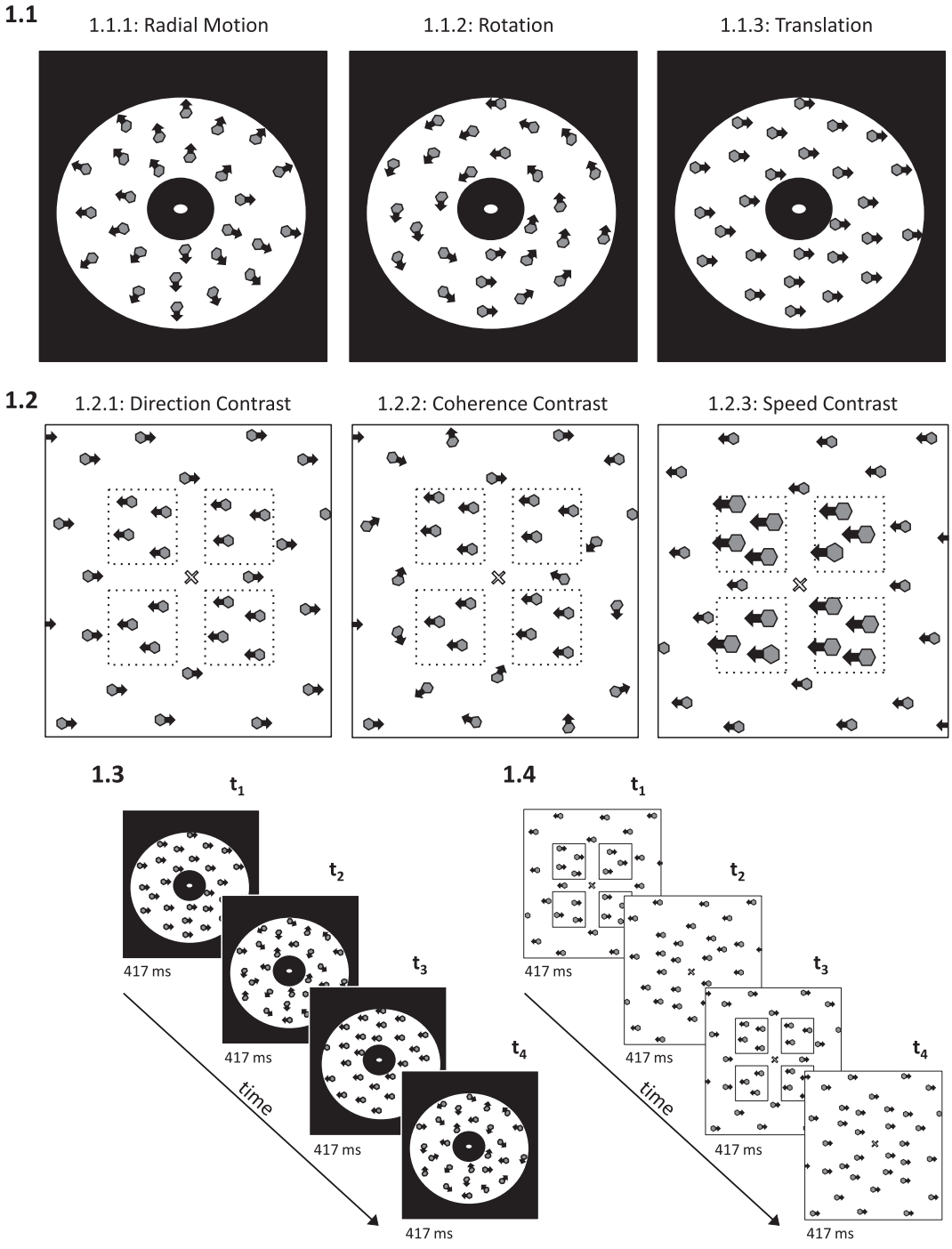

Fig. 1. Schematic representation of figure displays consisting of random dot motion. Experiment 1 stimuli consisted of global optic flow patterns, including radial motion (1.1.1), rotation (1.1.2), and linear translation (1.1.3). Experiment 2 stimuli consisted of 2D figures defined by motion contrast, including direction contrast (1.2.1), coherence contrast (1.2.2), and speed contrast (1.2.3). Illustrations 1.3 and 1.4 depict two respective display cycles for the two types of stimuli, including direction reversal. The optic flow displays modulated in time between a Coherent phase, in which the dot trajectories contributed to a global pattern of motion, and an Incoherent phase, in which the direction of dot motion was random. A full display consisted of 417 ms of Coherent and 417 ms of Incoherent motion, for a total of 833 ms per cycle. The motion contrast displays modulated in time between a Figure On phase, in which regional contrast was present, and a Figure Off phase, in which all dot motion settings were identical. A full display consisted of 417 ms of Figure On and 417 ms of Figure Off, for a total of 833 ms per cycle. For these displays, figure and background motion reversed in direction every other cycle.

mrCurrent (Smith-Kettlewell Eye Research Institute) software. The intensity values of these plots were normalized by harmonic, in order to illustrate the spatial distribution of the responses at each harmonic. Statistical significance of signal from noise was determined via a two-dimensional *t*-test called the T^2_{circ} (Victor & Mast, 1991).

2.1.5. Statistical analyses

All statistical analyses were conducted in R (version 2.15) using R-Studio (version 3.01). We employed a mass univariate approach to our data to test the effects of patterns and speed separately for each channel of interest (Blair & Karniski, 1993; Groppe, Urbach, & Kutas, 2011). Analyses of variance (ANOVA) were conducted to test

the effects of Pattern and Speed on the VEP signal. For Experiment 1, we report separate results for the 1F1 (modulation rate) and 1F2 (dot update rate) harmonics as well as the two intermodulation harmonics (1F1 − 1F2 and 1F1 + 1F2). We had no prior basis for predictions about 2F1 results for optic flow patterns, and thus do not report those results. For Experiment 2, we report all of these harmonics plus the 2F1.

The 35 channels of interest (see Fig. 2) were from occipital and parieto-occipital regions, chosen to permit comparisons with previous 5-channel SSVEP results (Gilmore et al., 2007; Hou et al., 2009) that measured activity at channels PO7, O1, Oz, O2, and PO8.

We report here the results of simple *F*-tests from illustrative channels. We chose an alpha level of 0.001 for our mass univariate analysis results to control for multiple comparisons. However, we occasionally mention effects that met less stringent criteria for significance to provide a fuller account of the data.

2.2. Results

Fig. 3.1 depicts an illustrative spectral plot of phase coherent amplitude responses averaged across occipital channels, which serves to represent the harmonics of interest in this experiment. Fig. 4 illustrates response amplitudes at 1F1 for speed groups 1 and 2, and Fig. 5 shows normalized 2D topographic plots of the spatial distribution of the 1F1 responses across sensor space. At 1F2, response amplitude increased with speed (see Fig. 6). Responses at 1F1 were strongest for the radial motion conditions for both groups. Also, overall, the 16 deg/s condition yielded the largest amplitudes across the pattern types. The topographic plots show strong responses to radial motion among lateral occipital channels at slower speeds, but the activity peak shifts to dorsomedial occipital channels at faster speeds. In contrast, rotation and translation have a similar focal medial occipital channels distribution at slow speeds, but at fast speeds exhibit a dorsomedial occipital distribution similar to responses for radial motion.

To quantify these effects, we ran statistical analyses as described previously. A preliminary test of the effect of speed group at 1F1 did not reach significance, $F(1,38) = 0.9$, *ns*, so we collapsed our subsequent analyses across the two groups in order to increase power. We then ran separate ANOVAs for the 35 channels of interest (see Fig. 7). At 1F1, significant pattern effects were observed among medial and right lateral channels (largest *F* was channel 72: $F(2,306) = 13.68$, $p < 0.001$), with radial motion yielding stronger responses than the other patterns (channel 72, rotation: $t(306) = -3.94$, $p < .001$; translation: $t(306) = -3.58$, $p < 0.001$). Medial channels also exhibited significant speed effects (largest *F* was channel 76: $F(4,306) = 5.09$, $p < .001$). Left lateral channels also showed effects of pattern, although most of the effects for these channels were only significant with an alpha criterion higher than 0.001. Similarly, weak linear trends across speeds ($ps < 0.01$) were observed among medial channels (71, 72, 75, 76, and 77).

For responses at 1F2, we found significant effects of speed in all channels tested (largest *F* was channel 85: $F(4,282) = 42.38$, $p < 0.001$), with significant linear trends observed across the speeds (largest *t* was channel 85: $t(282) = 6.11$, $p < 0.001$).

We also analyzed the results from the two sideband harmonics, 1F2 − 1F1 and 1F2 + 1F1, that reflect the degree to which global coherence modulations influenced the local motion/luminance dot update response. In both cases, while amplitudes were small, the results largely paralleled those found for the 1F2. Most of the channels showed significant effects of speed (1F2 + 1F1: channel 72: $F(4,298) = 41.92$, $p < 0.001$; 1F2 − 1F1: channel 76: $F(4,298) = 54.30$, $p < 0.001$), and the medial channels showed significant linear trends for speed (1F2 + 1F1: channel 71: $t(298) = 4.58$, $p < 0.001$; 1F2 − 1F1: channel 72: $t(298) = 4.96$, $p < 0.001$). For 1F2 + 1F1 (25.2 Hz), a few medial channels showed weak interaction effects (only channel 76 yielded a *p*-value below 0.001), indicating a difference in a linear trend across speeds for translation than for the other motion patterns.

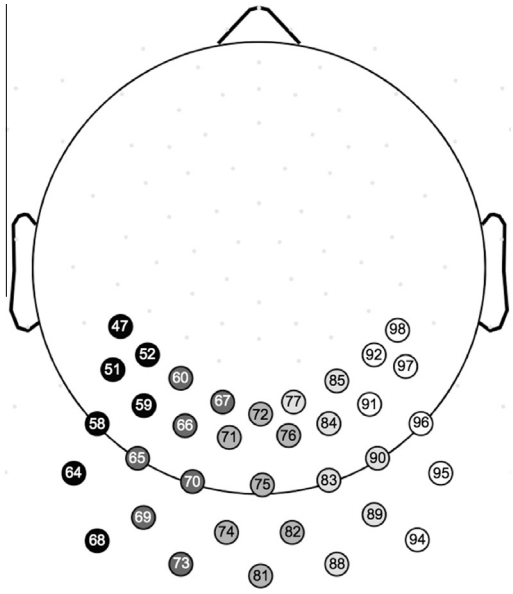

Fig. 2. Schematic representation of channels chosen for analysis. Channels were chosen for rough comparison of effects to previous experiments that employed low-density electrode montages (Gilmore et al., 2007; Hou et al., 2009). As our statistics focused on individual channels effects, the different shades of the channels in the display are not relevant to our design, but can cue viewers to a gross spatial organization for comparison with the 2D topographic plots (Figs. 5 and 9).

2.3. Discussion

The results of Experiment 1 indicate that evoked cortical responses corresponding to the temporal modulation of coherent global motion differ across patterns and speeds, though the effects vary by channel. At 1F1, responses in medial and lateral channels (especially right) were stronger for radial motion than for the other flow patterns. Interestingly, the topographic maps and amplitude plots suggest that the distribution of responses to radial motion differs across speeds. At slow speeds, the activity is bilateral, with the strongest activation in right lateral channels. At faster speeds, however, the distribution is dorsomedial. Responses to rotation and translation also show a shift of distribution across speeds, although the activity remains for the most part among medial channels. For all three patterns, amplitudes in medial channels increased as speed increased, and the responses looked quite similar at 16 deg/s. To our knowledge, this finding is novel. But, the result is generally compatible with prior low-channel count SSVEP results of Gilmore et al. (2007) and Hou et al. (2009). At fast (8 and 16 deg/s) speeds, however, responses looked increasingly similar, with dorsomedial occipital activation across all pattern types, perhaps reflecting pattern-general processing at these speeds. The dorsomedial response distribution at high speeds is compatible with the findings of Wattam-Bell et al. (2010), who used coherence modulations of global rotation at 8 deg/s, one of the faster speeds used here. Thus, what may have seemed like a discrepancy between the Gilmore et al. (2007) and Wattam-Bell et al. (2010) findings may instead reflect differential recruitment, due to parameter differences, of a circuits sensitive to different speed and global pattern combinations. The results also showed speed tuning at the 1F2 dot update rate, replicating previous results (Hou et al., 2009) with low-channel count electrode arrays. Interestingly, the speed

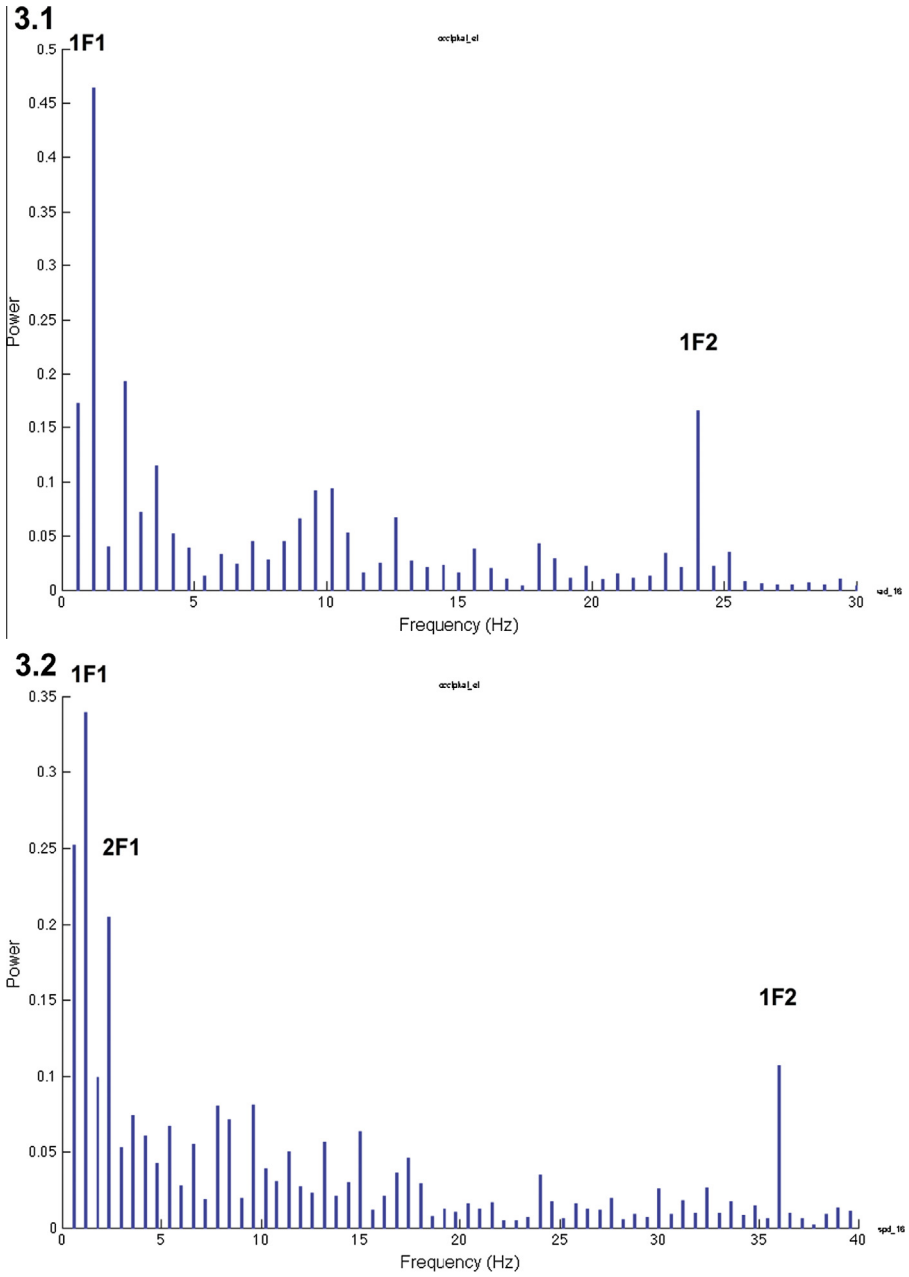

Fig. 3. Example spectral plots of group-averaged SSVEP responses for occipital channels for Experiment 1 (3.1) and Experiment 2 (3.2). The strongest responses were observed at the modulation rate of 1.2 Hz (1F1). Responses at the dot update rate (1F2) were small but significantly above noise. For Experiment 2, we also investigated 2F1 (2.4 Hz), for comparison with previous findings (Fesi et al., 2011).

tuning extended to the intermodulation harmonics, suggesting an interaction between global motion coherence and local motion/luminance responses.

The lateral activation pattern to slow radial motion may reflect activation in hMT or MST to the most dominant flow pattern of forward self-motion in depth (Britten, 2008; De Jong et al., 1994; Gibson, 1950). MST in particular has been shown to be important for detecting flow patterns associated with self-motion (Duffy & Wurtz, 1991, 1997; Huk, Dougherty, & Heeger, 2002; Komatsu & Wurtz, 1988; Newsome, Wurtz, & Komatsu, 1988; Perrone & Krauzlis, 2008; Tanaka & Saito, 1989; Thier & Erickson, 1992). If this is the case, the focal response at medial occipital cortex to slow rotation and translation could perhaps reflect processing related to flow components most likely imposed by head and eye movements, and less likely to reflect the structure of the environment (Britten, 2008; Lappe, 1998; Perrone & Krauzlis, 2008).

As for the dorsomedial occipital distribution of the responses at high speeds, Wattam-Bell et al. (2010) concluded that a similar response pattern reflected the activity of area V3a. This area, as well as surrounding area V7, regions of the intraparietal sulcus, V6, and the posterior cingulate, have been shown to be important for a multitude of functions related to depth processing (Backus et al., 2012; Caplovitz & Tse, 2007; Cottereau et al., 2011; Orban, 2011; Preston et al., 2008; Tsao et al., 2003), spatial attention (Behrmann, Geng, & Shomstein, 2004; Bisley & Goldberg, 2003; Culham et al., 2012; Tootell et al., 1998), motor intentions (Andersen et al., 1997; Astafiev et al., 2003; Nakamura et al., 2001; Rizzolatti, Fogassi, & Gallese, 1997) and navigation (Bremmer, 2005; Cardin et al., 2012; Harvey, Braddick, & Cowey, 2010; Kriegeskorte et al., 2003; Fischer et al., 2012). This dorsomedial distribution is also quite similar to that of the 1F1 response to the onset of motion-defined figure contrast reported by Fesi et al.

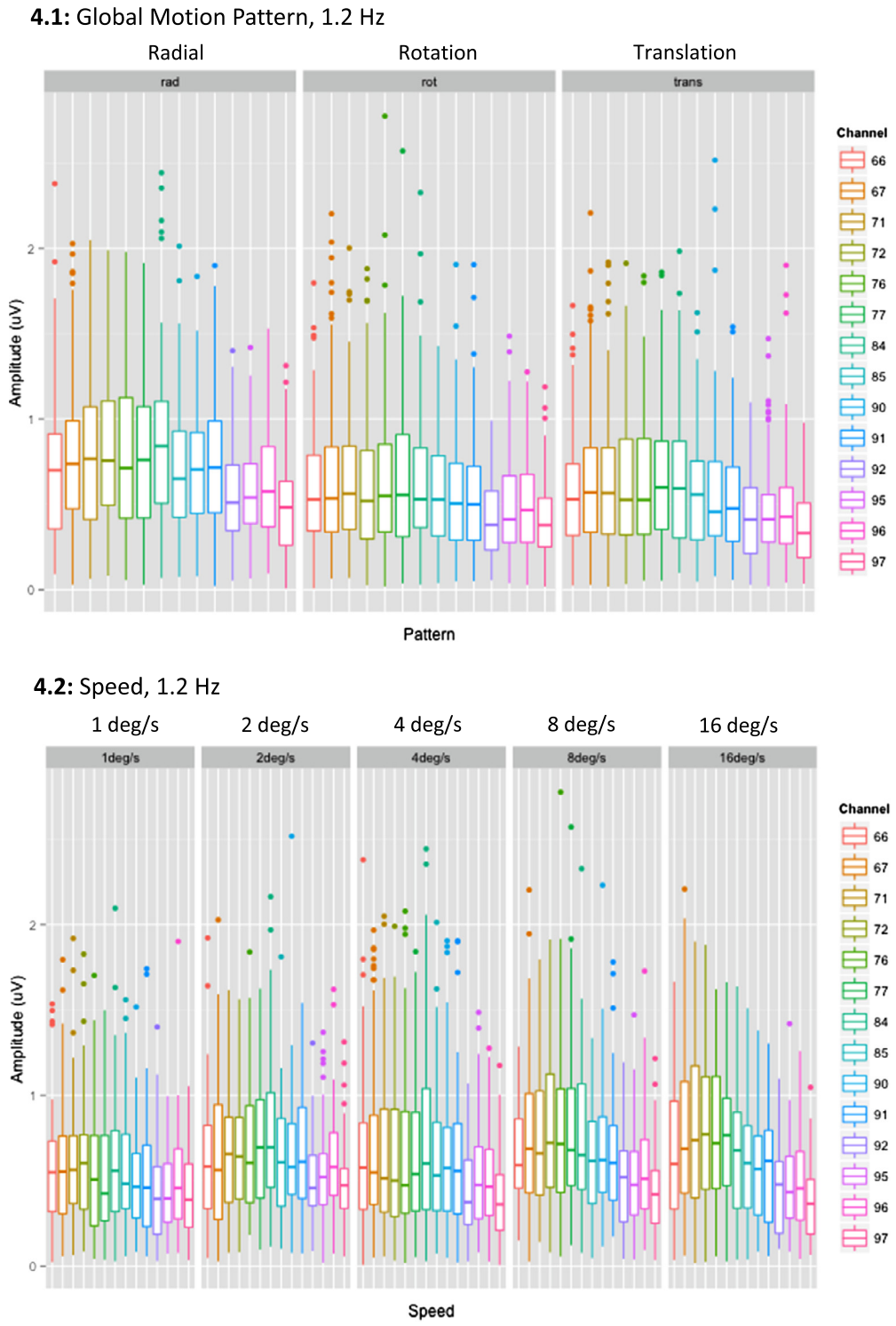

Fig. 4. Amplitude plots for responses at 1F1 (1.2 Hz) for channels that showed significant effects ($p < 0.001$). Responses are shown across patterns (4.1) and speed (4.2). Responses were strongest for radial motion. At fast speeds, the responses were strong among medial channels.

(2011). If this reflects activity in the same or shared cortical regions, it may speak to a common role of these areas of tracking in depth and spatial attention. If this is the case, the pattern-general response observed here may not reflect the processing of ego-motion *per se*, but could instead reflect sensitivity to changes in the depth structure of a scene.

Because of the poor spatial resolution of EEG recorded from the scalp, the precise cortical sources of these evoked responses cannot be determined. However, the results of the study clearly demonstrate that normal adult cortical processing of optic flow, and the global space–time sensitivity of the underlying mechanisms, is more complex than had been assumed in previous studies (Hou et al., 2009; Wattam-Bell et al., 2010). Namely, optic flow engages a network of systems beyond lateral regions such as MT and MST. This has important implications for understanding both adult function and the development of global motion sensitivity.

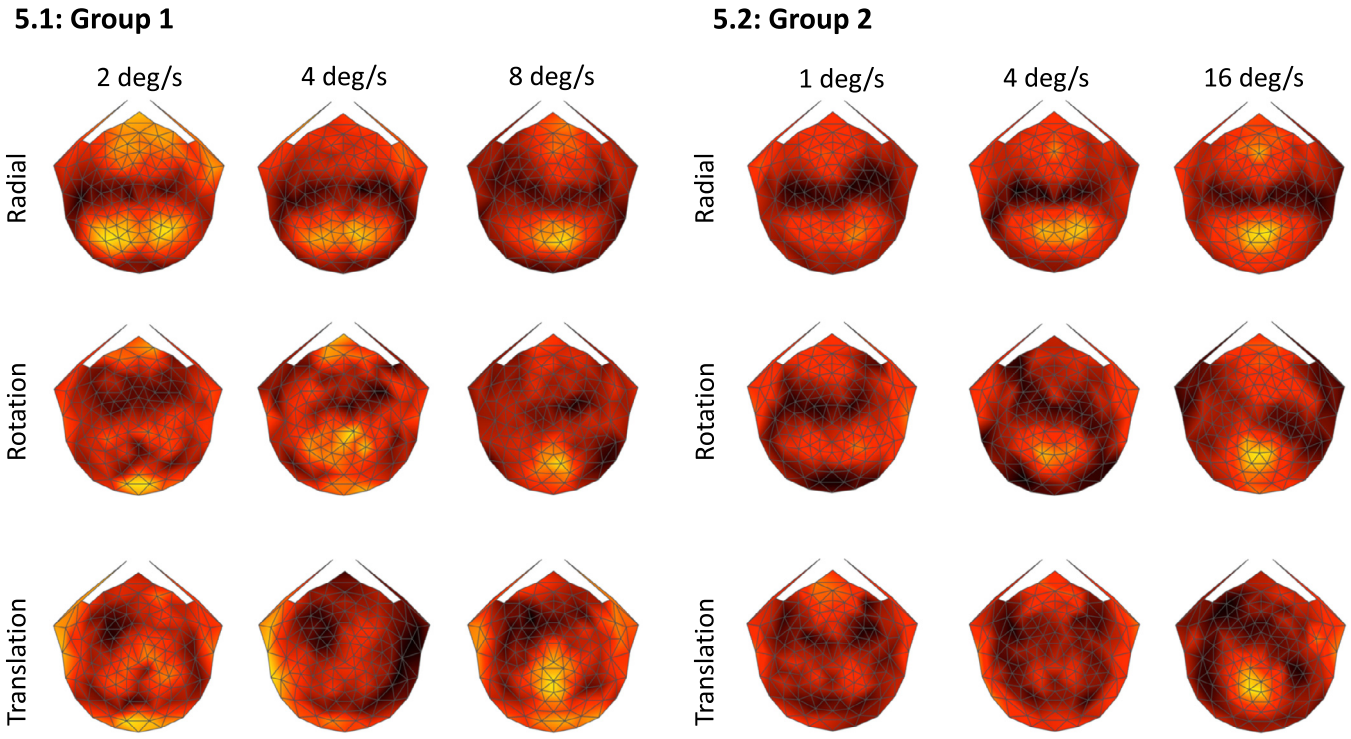

Fig. 5. 2D topographic maps of SSVEP responses of Groups 1 and 2 at 1.2 Hz (1F1) across patterns and speeds. The intensity values of the 2D scalp plots were normalized for each pattern at 1F1, so as to best illustrate the spatial distribution of responses across speeds. At fast speeds, responses for all patterns show a similar dorsomedial distribution. At slow speeds, responses to radial motion are bilaterally distributed, while responses to the other two patterns are at a more focal medial locus.

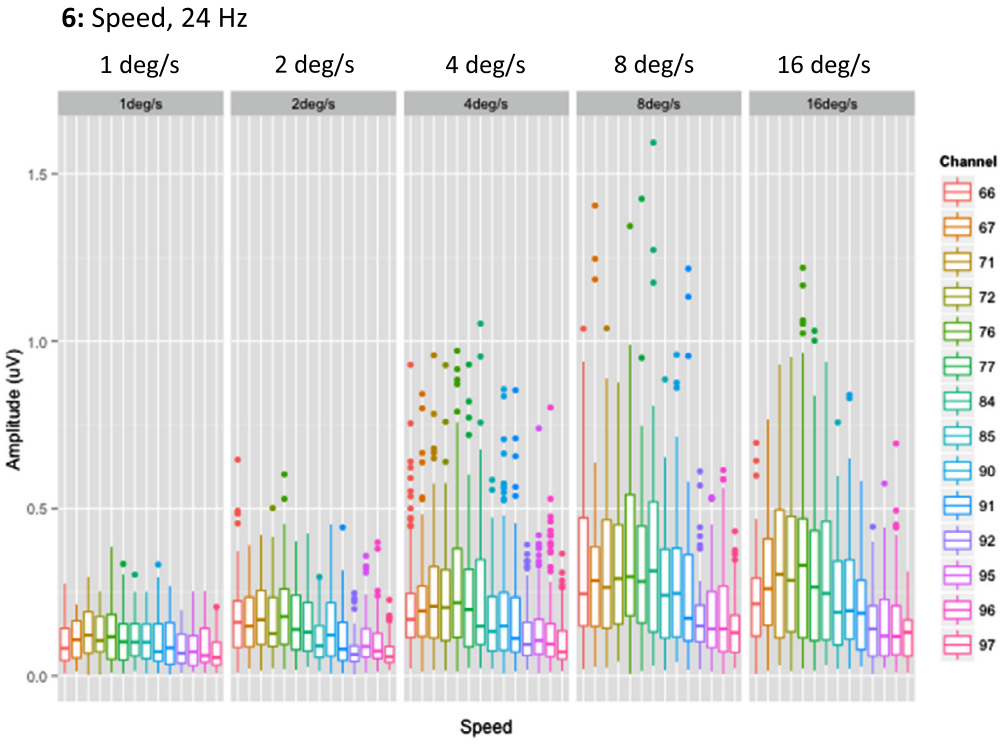

Fig. 6. Amplitudes of responses at 1F2 (24 Hz) for channels that showed significant speed effects ($p < 0.001$). The channel responses are plotted across speeds, demonstrating a prominent increase in amplitude with speed.

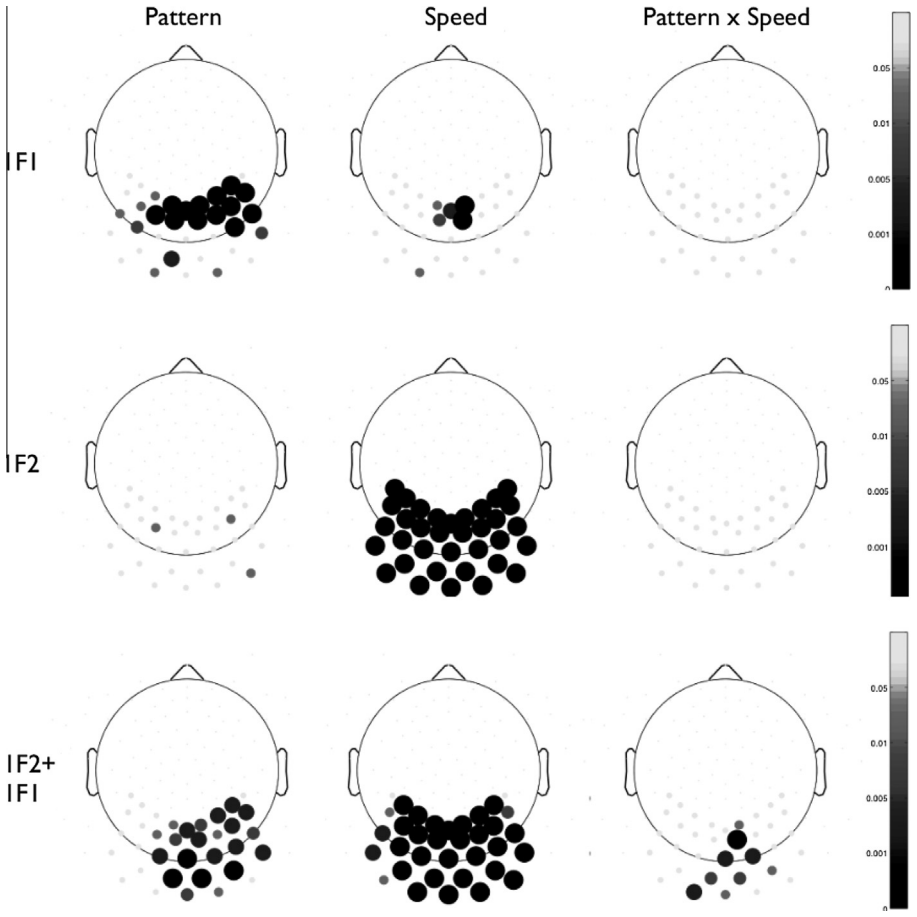

Fig. 7. Statistical results for Experiment 1. The 2D channel maps plot the results from the analyses run separately for each channel. The size and darkness of the circles indicate the lowest alpha value for which the result of a channel met statistical significance. The maps show the results for each effect and interaction (left to right) and at each harmonic of interest (top to bottom).

3. Experiment 2: motion-defined figures

3.1. Methods

3.1.1. Participants

20 adults (10 female; mean age: 19.5 years) participated in Experiment 2. Subjects were research assistants who had volunteered to participate, or were recruited from an undergraduate subject pool for research credit. All subjects had normal or corrected-to-normal vision, as determined by a brief evaluation of binocular Snellen optotype acuity.

3.1.2. Display

Monitor and display settings were similar to those of Experiment 1, with some exceptions. Displays featured a uniform linear dot motion background region alternating with four 9° × 9° figure regions at 1.2 Hz. The figure regions were defined by a motion contrast (see Fig. 1.2) relative to the surround. The square figures moved across the screen according to a particular dot displacement setting per condition. A full display cycle consisted of 833 ms of figure on/figure off modulation. The direction of dot motion reversed every other cycle to control for adaptation of direction-sensitive cells. For compatibility with previous experiments on motion-defined figures (Fesi et al., 2011), a display area of 28° by 28° was used. The dot update rate was 36 Hz.

All subjects viewed three motion contrast types (direction, global coherence, speed) at three different speed settings. Dot displacements were: 3.5, 7, and 27 arcmin per dot update (yielding speeds of 2.1, 4.2, and 16.2 deg/s, respectively at the 36 Hz update frequency). Each subject viewed a total of 9 conditions, and 10 trials were recorded per condition (yielding a total of 90 trials per subject session). Direction-defined figures differed by moving 180° opposite to the background. Coherence-defined figures differed by appearing at 0% coherence (incoherent) against a 100% coherent background. Speed-defined figures moved at 4.2 deg/s faster than the uniformly moving background.

3.1.3. Procedure

Procedures and VEP analysis were identical to those of Experiment 1.

3.2. Results

Fig. 3.2 depicts a representative spectral plot from occipital channels. Fig. 8 shows response amplitudes at 1F1 and 2F1, while Fig. 9 shows topographic plots of the distribution of responses at these harmonics. Fig. 10 shows channel responses at 1F2 that showed significant effects of speed. Similar to Experiment 1, responses at this harmonic increased in amplitude with speed.

As with Experiment 1, we ran separate ANOVAs for 35 channels to quantify the observed effects (Fig. 11). At 1F1 we found significant interactions of Pattern by Speed among dorsomedial channels (largest F was channel 77: $F(4,152) = 8.24$, $p < 0.001$), while most occipital channels showed significant pattern effects (largest F was channel 74: $F(2,152) = 18.34$, $p < 0.001$), and weaker speed effects ($ps < .01$ and $ps < 0.05$). For the channels with a statistically

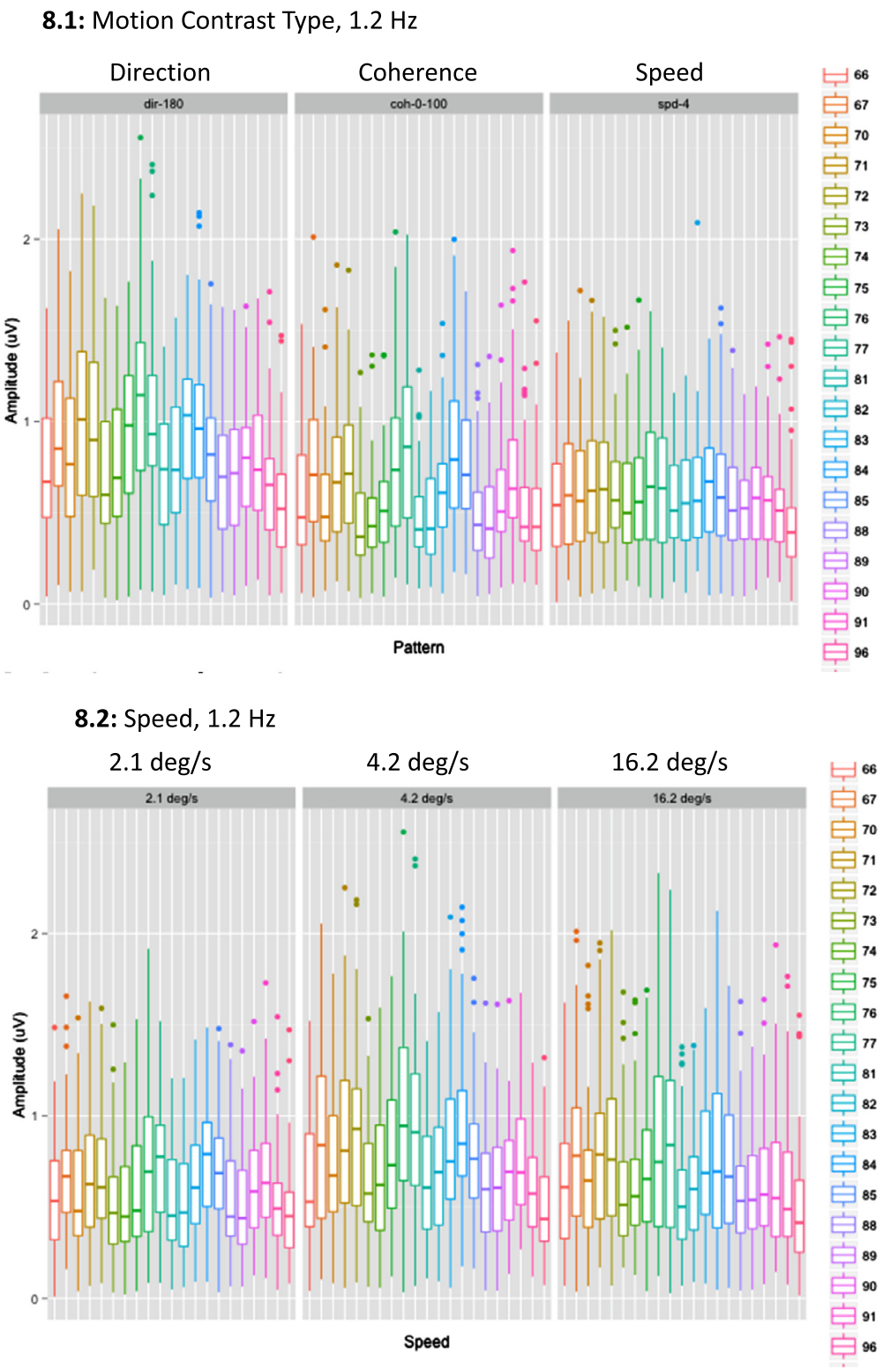

Fig. 8. Amplitudes of responses for channels that showed significant effects ($p < 0.001$). Channel amplitudes for responses at 1F1 are shown across motion contrast types (8.1) and speeds (8.2), as are those for responses at 2F1 (8.3 and 8.4, respectively). Responses at 1F1 were strongest among medial channels, particularly for direction contrast. At 2F1, responses look more lateralized, particularly at 4 deg/s.

significant pattern effect, direction contrast yielded stronger responses than coherence and speed (channel 74, coherence contrast: $t(152) = -6.03$, $p < 0.001$; speed contrast: $t(152) = 3.54$, $p < 0.001$), although for some channels (73 and 95), the difference between direction and speed contrast was only significant at a more liberal threshold ($ps < 0.05$). Among the channels with significant effects of speed, all showed strong to weak linear trends, and a few (81 and 82) showed weak quadratic trends ($ps < 0.01$). Among the channels with significant interactions, almost all showed a significant difference between linear speed trends for direction contrast versus speed contrast (channel 77: $t(152) = -4.033$, $p < 0.001$). Consistent with these results, the

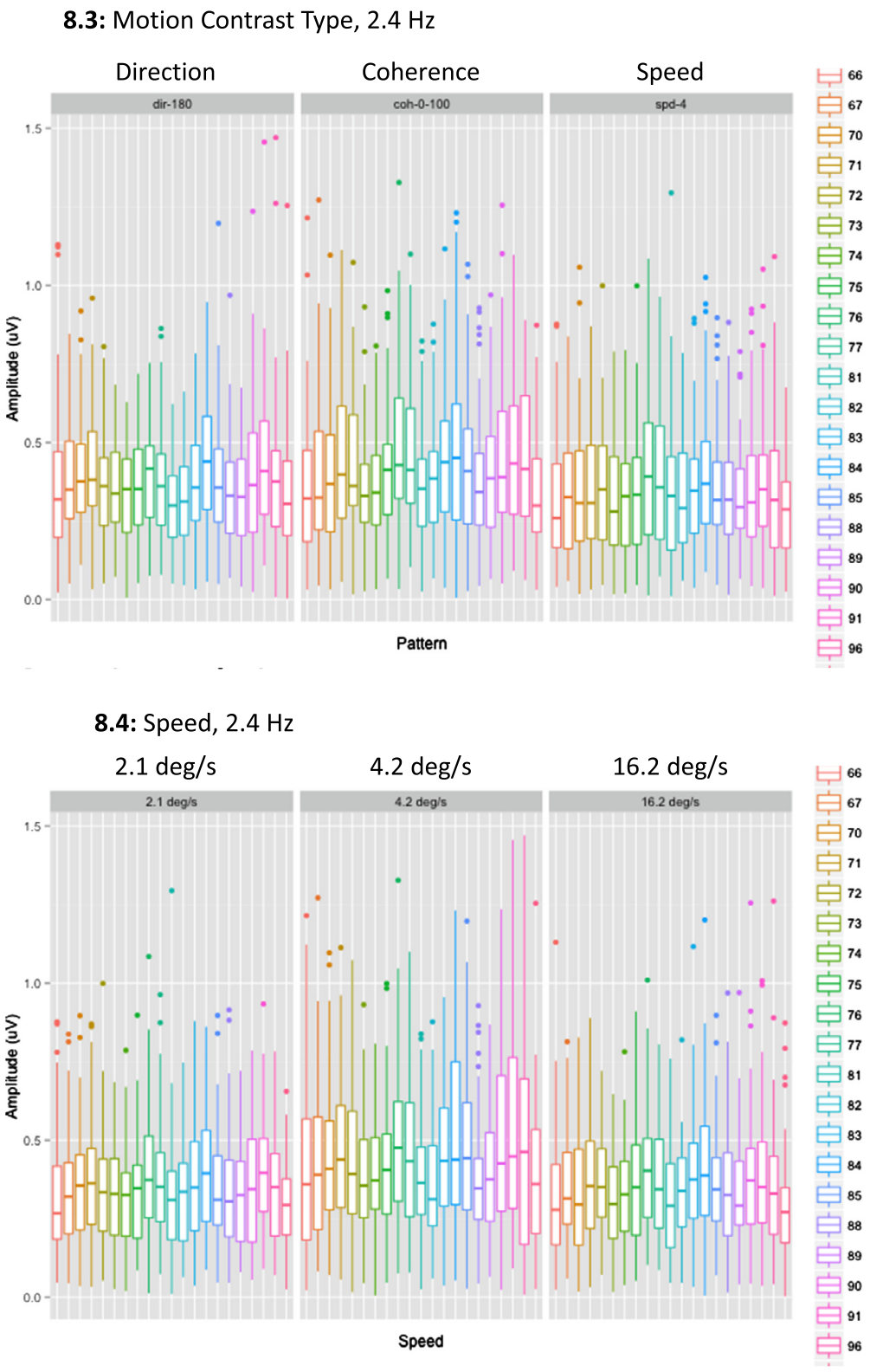

Fig. 8 (*continued*)

amplitude plots reveal that, among medial channels, responses were strongest for direction contrast for all speeds except for 4 deg/s. At this speed, the figures defined by speed contrast yielded the strongest responses overall. For all of the patterns, the responses were strongest at 4 deg/s, perhaps reflecting the quadratic trend, yet the amplitudes did not decrease much at 16 deg/s, thereby enabling significant linear trends as well.

At 2F1, we found significant effects of speed in right lateral channels (highest F was channel 91: $F(2,152) = 9.15$, $p < 0.001$), and weaker effects of speed in left lateral channels ($ps < 0.01$ and $ps < 0.05$). None of these channels showed significant linear trends, although three channels towards the right of the scalp (76, 92, and 98) showed significant interactions ($ps < 0.05$), where quadratic trends for direction differed from those for coherence contrast

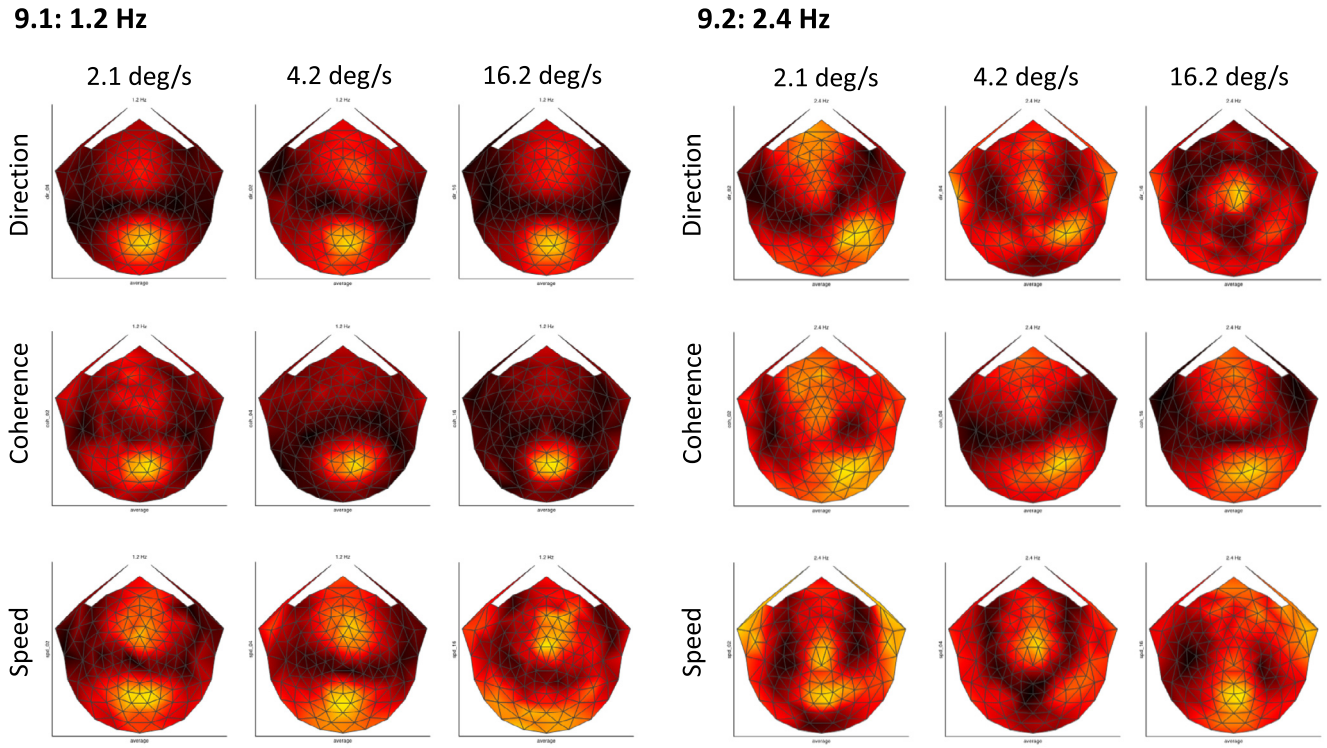

Fig. 9. 2D topographic maps of SSVEP responses to modulations of motion contrast. At 1F1 (9.1), responses to direction contrast and coherence contrast show very similar dorsomedial distributions, while responses to speed contrast look similar at the slower speeds, but not at 16 deg/s. Additionally, the speed contrast responses show an anomalous locus at centrofrontal channels. At 2F1 (9.2), responses to direction and coherence are similarly bilateral (though the trend is not as robust for direction at the fastest speed), while responses to speed contrast again are similar only at the slower speeds.

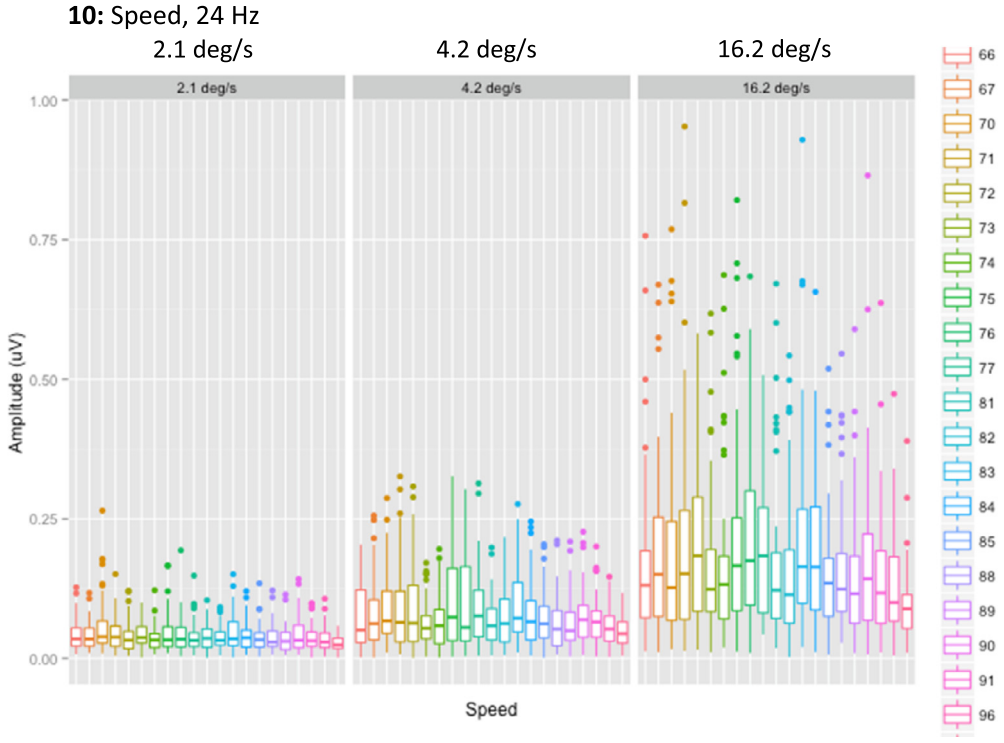

Fig. 10. Amplitudes of responses at 1F2 (36 Hz) for channels that showed significant speed effects ($p < 0.001$). The amplitudes show monotonic tuning to dot speed, similar to what has been observed in Experiment 1 and by Hou et al. (2009) for global coherence modulations of optic flow.

($ps < 0.05$). Weak effects of pattern were also found among right lateral channels ($ps < 0.05$), with coherence contrast yielding stronger responses at this harmonic.

At 1F2 we found significant effects of speed for all of the tested channels (highest F was channel 77: $F(2,152) = 90.78$, $p < 0.001$), with significant linear trends across speeds (channel 77:

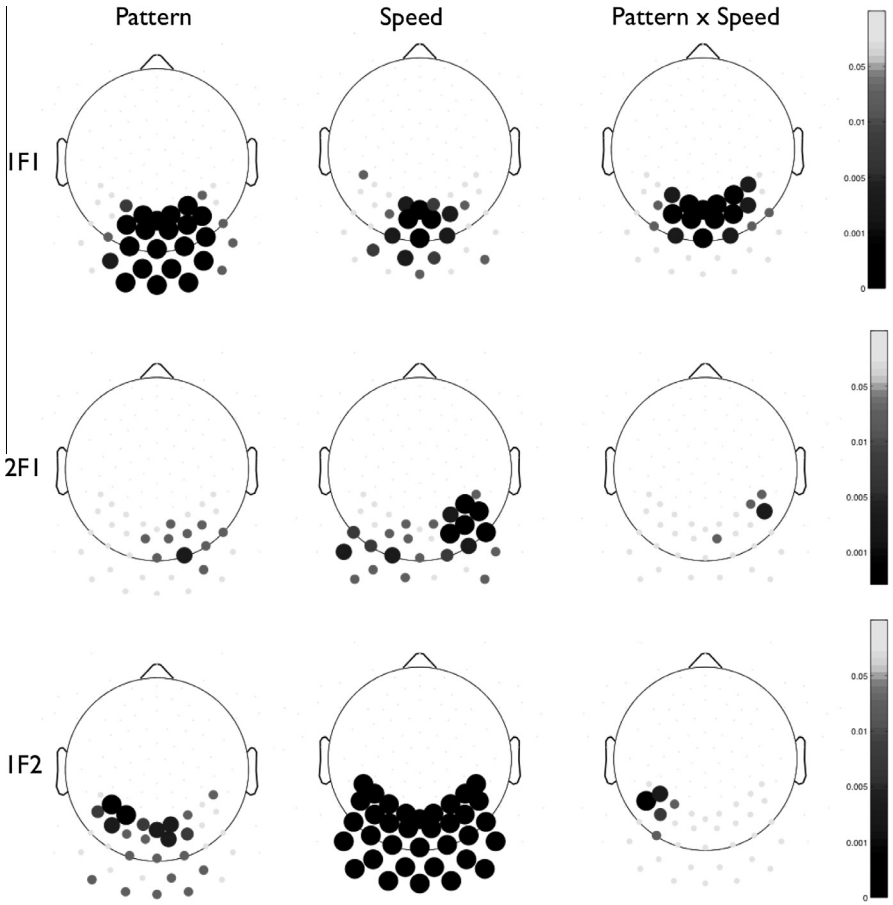

Fig. 11. Statistical results for Experiment 2. The 2D channel maps plot the results from the analyses run separately for each channel. The size and darkness of the circles indicate the lowest alpha value for which the result of a channel met statistical significance. The maps show the results for each effect and interaction (left to right) and at each harmonic of interest (top to bottom).

$t(152) = 8.32$, $p < 0.001$). However, some left lateral channels (51, 52, 59, 60, and 65) also yielded weak Pattern by Speed interactions that indicate differences in linear trends across speeds for coherence contrast versus the other patterns ($ps < 0.05$). Additionally, a few channels (51, 52, 59, 71, 72, 76, and 77) yielded weak effects of pattern ($ps < 0.05$), with coherence contrast yielding weaker responses than the other patterns. The intermodulation harmonics also showed significant interactions among medial channels (1F2 + 1F1: channel 91: $F(4,152) = 6.64$, $p < 0.001$; 1F2 − 1F1: channel 76: $F(4,144) = 8.37$, $p < 0.001$), but with linear trends for speed contrast differing from the other patterns ($ps < 0.01$), similar to the 1F1 responses.

3.3. Discussion

The spatial distribution of the 1F1 and 2F1 responses for the direction and coherence conditions were similar to those observed by Fesi et al. (2011). The 1F1 response, which corresponds to the onset (or offset) of figures defined by motion contrast (Fesi et al., 2011), had a dorsomedial occipital distribution in both studies. Amplitudes at this harmonic were stronger for direction contrast than for the other patterns for most speeds, except for responses to speed contrast at 4 deg/s. Across all patterns, the responses at 1F1 seemed to peak at 4 deg/s, although the differences between 4 deg/s and 16 deg/s were not great. The direction- and coherence-defined figures exhibited similar tuning patterns, with 1F1 responses peaking at the middle speed of 4 deg/s and then saturating. The 2F1 response corresponds both to the onset and offset of a motion-defined figure. Here it had a bilateral occipital distribution, with direction patterns eliciting more focally bilateral sites than coherence, although there was some change in distribution across speeds here. At this harmonic, responses were strongest for coherence contrast, particularly among medial and right lateral channels. Although there were some distinguishing characteristics between responses for the two figure types, the data here were similar to the trends reported by Fesi et al. (2011), and show substantially less variation across patterns than the data of Experiment 1. The results support the claim that motion-defined figure mechanisms are largely cue-invariant, at least where direction or global motion coherence is concerned.

The data for speed-defined figures, however, exhibited some differences. There were some similarities across all figure types: for the slower two of the three speed conditions, the amplitudes and spatial distributions among occipital electrodes were very similar to those of the direction and coherence-defined figures. Additionally, the distribution of activity for the fastest condition was roughly similar to the other conditions, although the 2F1 response was somewhat more diffuse than the other conditions. With regard to amplitudes, however, statistical tests reveal that the tuning across speeds for speed contrast was different from the direction and coherence contrast conditions. Moreover, a centro-frontal distribution was observed for all three speed contrast conditions. This centro-frontal activation may reflect activity in the frontal eye fields (FEF), a region known to be important for eye movements including smooth pursuit (Gottlieb, Macavoy, & Bruce, 1994; MacAvoy, Gottlieb, & Bruce, 1991; Petit et al., 1997), which has been implicated in segmentation in depth via motion parallax (Naji & Freeman, 2004; Nawrot, 2003a, 2003b; Nawrot & Joyce,

2006; Nawrot & Stroyan, 2009, 2012; Wexler & van Boxtel, 2005). However, the spatial resolution of the methods used here were not sufficient to localize the source of our data, and so this possibility must be examined in future research.

As in Experiment 1, our 1F2 and intermodulation harmonic results showed a complex pattern of speed tuning for different types of motion-defined forms, suggesting significant interaction among local motion/luminance dynamics and those associated with global edge/shape/form processing.

4. General discussion

4.1. Summary of findings

These experiments investigated the sensitivity and spatial distribution of VEP responses to optic flow and motion-defined figure patterns across speeds. Experiment 1 showed that coherence-modulating radial motion patterns elicited the strongest responses overall, compatible with previous findings in adults (Gilmore et al., 2007). A significant pattern by speed interaction was observed, suggesting a pattern-specific speed sensitivity for optic flow stimuli. At 2 deg/s, radial patterns elicited the strongest responses, particularly among lateral channels. At 8 and 16 deg/s, however, each pattern elicited similar dorsomedial occipital activity. This finding was not expected, but indicates that the spatial distribution and response sensitivity for coherent optic flow varies depends upon pattern type as well as speed. Furthermore, the results seem to resolve what had previously seemed to be conflicting interpretations of global motion processing in adults by Gilmore et al. (2007) and Wattam-Bell et al. (2010). Gilmore et al. (2007) highlighted a medial-to-lateral shift in response locus across the age groups, while Wattam-Bell et al. (2010) suggested a lateral-to-dorsomedial shift with age. Both studies used fixed speeds across conditions, with the former using displays moving at 5.5 deg/s, and the latter using displays moving at 8 deg/s. Because we varied speed as well as flow patterns here, we have observed response distributions that are compatible with both studies. Thus, Gilmore et al. (2007)'s lateral response bias for radial motion may only occur at slower speeds, and Wattam-Bell et al. (2010)'s dorsomedial response to global rotation may only occur at faster speeds.

Importantly, our results indicate that cortical processing of global motion engages a more widespread network with more complex space and pattern tuning properties than had previously been assumed. Attempts to understand the development of cortical sensitivity should therefore consider the importance of the parameters used even for adult electrophysiological data, as well as brain mapping studies that implicate multiple brain areas in optic flow, depth, and navigation (Backus et al., 2012; Bremmer, 2005; Caplovitz & Tse, 2007; Cardin et al., 2012; Cottereau et al., 2011; Fischer et al., 2012; Harvey, Braddick, & Cowey, 2010; Kriegeskorte et al., 2003; Morrone et al., 2000; Orban, 2011; Preston et al., 2008; Tsao et al., 2003).

Experiment 2 compared speed sensitivity of responses across patterns of motion-defined figures. The observation of two responses to the patterns—one for contrast onset at dorsomedial channels, and one for both onset and offset at lateral channels—largely replicated the findings of Fesi et al. (2011). In addition, the spatial distribution and speed tuning of the responses were more consistent across motion-defined figure types than that for optic flow patterns. Figures defined by speed contrast, however, may be an important exception: the spatial distribution was somewhat distinct for this figure type, particularly responses at centro-frontal channels. This case needs to be more fully explored in the future.

As a whole, the results provide insights into integrative global motion processing in the adult brain and have important implications for investigations of how these mechanisms develop.

4.2. Integration of findings

While the two experiments are independent of one another, they may collectively provide evidence of shared processing mechanisms between self- and object-motion systems. For instance, the bilateral response to the onset and offset of figural motion contrast may reflect activity in hMT, which has been implicated in segmentation as well as global motion integration (Born et al., 2000; Likova & Tyler, 2008; Majaj et al., 2007; Marcar et al., 1995; Pack, Gartland, & Born, 2004). The results from a separate study (Fesi et al., unpublished) indicate that bilateral 2F1 responses to motion-defined figures are weighted by the global coherence of local motion vectors, a property attributed to MT (Braddick, 1993; Movshon & Newsome, 1996; Newsome & Pare, 1988; Stoner & Albright, 1992; though see Majaj et al., 2007). A similar bilateral occipital activation was also observed for radial motion in Experiment 1. If the lateralized responses to optic flow and motion-defined figures both reflect hMT activity, this would illustrate differential processing of patterns within a common cortical region, a notion compatible with multiple findings regarding the role of MT (e.g., Likova & Tyler, 2008; Krug & Parker, 2011; Morrone et al., 2000).

However, it is also possible that this similar bilateral activation actually reflects distinct but closely neighboring areas rather than a common mechanism. The bilateral responses to motion-defined figures could instead reflect activity from the lateral occipital (LO) complex, a subset of regions collectively regarded as important for object processing that has exhibited cue-invariant sensitivity to object-related information (Appelbaum et al., 2006; Ferber, Humphrey, & Vilis, 2003, 2005; Grill-Spector, Kourtzi, & Kanwisher, 2001; Grill-Spector et al., 1999; Stanley & Rubin, 2003). Interestingly, the LO-complex has previously been shown to exhibit a categorical sensitivity to parametrically varied cues to depth structure (Preston et al., 2008), similar to the response tuning observed by Fesi et al. (2011) among lateral occipital channels across magnitudes of motion contrast. Other studies have suggested that the LO-complex demonstrates a similar categorical sensitivity for texture contrast (Thielscher et al., 2008) and object size (Altschuler et al., 2012; Mendola et al., 1999). It's therefore possible that the bilateral activation at 2F1 to motion-defined figures observed by Fesi et al. (2011) and here in Experiment 2 reflects activity in the LO-complex instead of hMT.

Possible evidence for another common mechanism for optic flow and motion-defined figure processing is the dorsomedial occipital activation observed for both experiments. In Experiment 1, this activation was observed for the onset of globally coherent motion across all pattern types at fast speeds. In Experiment 2, this was observed for contrast onset, and has been shown to exhibit sensitivity to the magnitude of motion contrast (Fesi et al., 2011). Metric sensitivity to depth related information has previously been observed in dorsomedial occipital regions V3a, V7, and IPS (Preston et al., 2008). V3a has been associated with a number of functions related to changes in global depth structure (Caplovitz & Tse, 2007; Cottereau et al., 2011; Tootell et al., 1998; Tsao et al., 2003), yet was also cited by Wattam-Bell et al. (2010) as a locus for adult global motion processing. V7 and IPS are also important for processes related to depth (Bremmer, 2005; Cottereau et al., 2011; Orban, 2011; Peuskens et al., 2001; Preston, Kourtzi, & Welchman, 2009; Theys et al., 2012; Wexler & van Boxtel, 2005), and IPS is important for spatial attention and motor planning (Astafiev et al., 2003; Behrmann, Geng, & Shomstein, 2004; Bisley & Goldberg, 2003; Culham et al., 2012;

Nakamura et al., 2001; Rizzolatti, Fogassi, & Gallese, 1997). Because we used moving figures for our motion contrast displays, the 1F1 responses in Experiment 2 may reflect a sensitivity to steady changes in global depth structure rather than motion contrast onset *per se*. A plausible interpretation for this common dorsomedial activation, then, is that all of the patterns recruit areas important for depth and spatial attention. For the optic flow patterns, this may be related to steering and navigation; for the motion-defined figures, this may be related to tracking a moving object's position in depth.

Finally, both experiments yielded responses to modulations of various integrative properties that were distinct from the response at the dot update rate, 1F2. The 1F2 response has been used to test for differential sensitivity to local versus global motion (Gilmore et al., 2007; Hou et al., 2009; Weinstein et al., 2011). In the current study, the focal distribution of the 1F2 response at medial occipital channels looks similar across the various patterns and speeds used (see Fig. 12). This similarity supports the notion that the 1F2 response reflects basic visual processing in V1, rather than an area sensitive to integrative motion properties. There is some evidence suggesting that the 1F2 response is sensitive to luminance changes that are not strictly motion-related as well as to motion (Gilmore et al., 2011). However, the 1F2 responses in Experiments 1 and 2 increased with dot speed (see Figs. 6 and 11) as previously reported by Hou et al. (2009). We also found evidence in the amplitude patterns of the intermodulation harmonics (1F2 ± 1F1) that local motion/luminance and global coherence/form signals interact, similar to results others have observed (e.g., Appelbaum et al., 2006) in situations where attention is manipulated.

4.3. Limitations

Our use of non-invasive electrophysiological measures means that a satisfactory localization of function in the brain was not possible here. Nevertheless, the experiments here offer insights into the response properties of adult human cortex to different categories of complex motion, and can be readily compared to similar data from nonverbal populations such as infants and non-human primates. It will be necessary, however, to utilize a method with fine spatial precision in order to authoritatively localize the responses reported here to specific regions of cortex.

Another limitation is the reliance upon the passive, centrally fixated viewing of stimuli—particularly patterns that are presumed to be important for action. The problems of restricted viewing, however, are not unique to EEG: they extend to most neurophysiological recording methods, including fMRI, where participants need to view displays while lying on their backs, remaining as still as possible. The use of human observers to monitor eye movements rather than eye tracking equipment is another limitation. While we have no evidence that eye movements contaminated our results, we cannot rule out the possibility conclusively. Future studies that more precisely measure eye position and control for changes in position may be necessary to understand all of the data patterns presented here.

4.4. Conclusion

Cortical responses to optic flow vary substantially across patterns and speeds. Previous studies used only one pattern to assess speed sensitivity of a general global motion mechanism, yet these

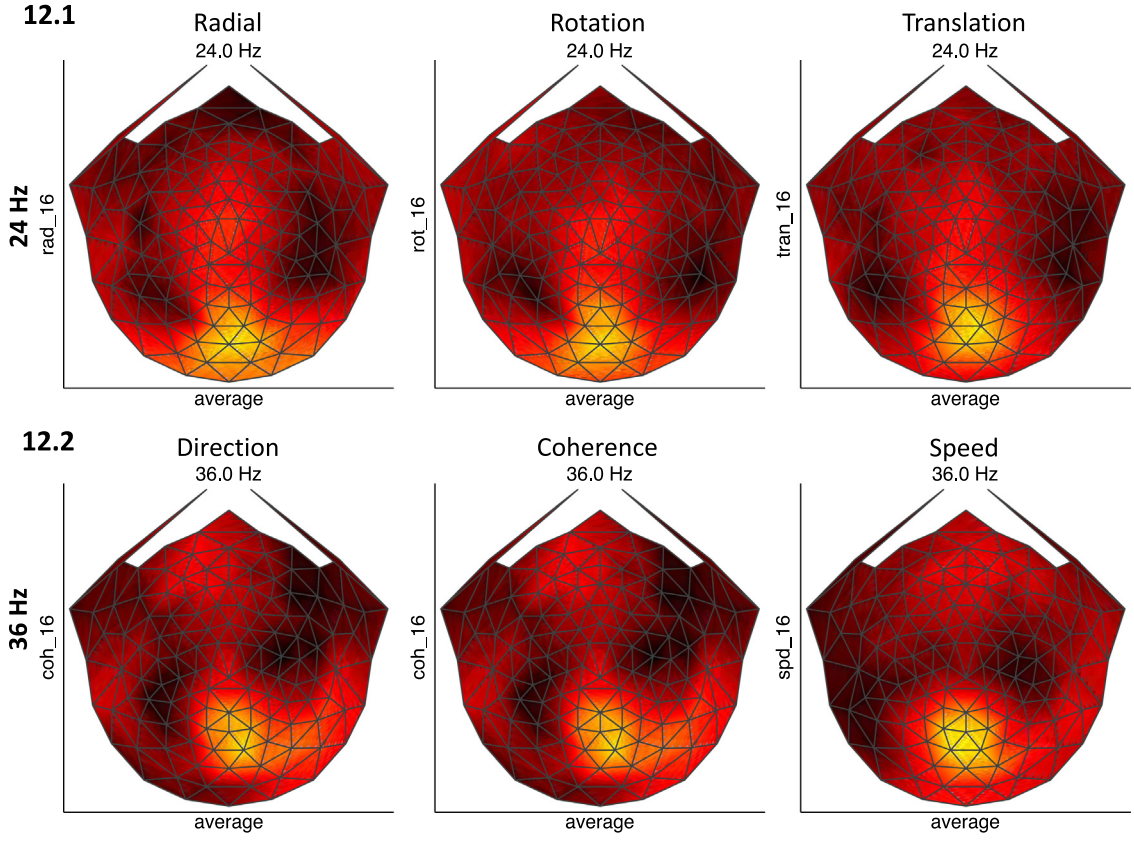

Fig. 12. Example 2D topographic maps of SSVEP responses at 1F2 to coherence modulations of global optic flow (12.1) and modulations of regional motion contrast (12.1), provided to show the similar spatial distribution of the dot update response across patterns. All plots correspond to the fastest speed used in each experiment, because the 1F2 has been shown to modulate with dot speed (see Figs. 6 and 10).

results indicate that separate mechanisms are differentially recruited depending on pattern and speed. At high speeds, the responses seem pattern-general, but distinct space–time integration thresholds across the patterns highlights crucial processing differences even from this pattern-general mechanism. The processing of motion-defined figures is comparatively more uniform, although the unique trends for speed-defined figures qualify the extent to which figure processing is cue-invariant. Moreover, the experiments have revealed some possible common mechanisms for the two pattern classes, not only for global motion integration, but also for depth and spatial attention. Finally, the experiments' use of steady-state visual evoked potential recording methods to assess cortical sensitivity provides a body of data that is readily comparable with infants, children, and animals. Thus, the results of these experiments provide an important reference for any future studies on normal or abnormal development, or general animal processing of integrative motion patterns.

References

Altschuler, T. S., Molholm, S., Russo, N. N., Snyder, A. C., Brandwein, A. B., Blanco, D., et al. (2012). Early electrophysiological indices of illusory contour processing within the lateral occipital complex are virtually impervious to manipulations of illusion strength. *NeuroImage, 59*(4), 4074–4085. http://dx.doi.org/10.1016/j.neuroimage.2011.10.051.

Andersen, R., Snyder, L. H., Bradley, D. C., & Xing, J. (1997). Multimodal representation of space in the posterior parietal cortex and its use in planning movements. *Annual Review of Neuroscience, 20*, 303–330. http://dx.doi.org/10.1146/annurev.neuro.20.1.303.

Appelbaum, L. G., Wade, A. R., Vildavski, V. Y., Pettet, M. W., & Norcia, A. M. (2006). Cue-invariant networks for figure and background processing in human visual cortex. *Journal of Neuroscience, 26*(45), 11695–11708.

Astafiev, S. V., Shulman, G. L., Stanley, C. M., Snyder, A. Z., Van Essen, D. C., & Corbetta, M. (2003). Functional organization of human intraparietal and frontal cortex for attending, looking, and pointing. *Journal of Neuroscience, 23*(11), 4689–4699.

Backus, B. T., Fleet, D. J., Parker, A. J., & Heeger, D. J. (2012). Human cortical activity correlates with stereoscopic depth perception. *Journal of Neurophysiology*, 2054–2068.

Behrmann, M., Geng, J. J., & Shomstein, S. (2004). Parietal cortex and attention. *Current Opinion in Neurobiology*. http://dx.doi.org/10.1016/j.conb.2004.03.012.

Berzhanskaya, J., Grossberg, S., & Mingolla, E. (2007). Laminar cortical dynamics of visual form and motion interactions during coherent object motion perception. *Spatial Vision, 20*(4), 337–395. http://dx.doi.org/10.1163/156856807780919000.

Bisley, J. W., & Goldberg, M. E. (2003). Neuronal activity in the lateral intraparietal area and spatial attention. *Science, 299*(5603), 81–86. http://dx.doi.org/10.1126/science.1077395.

Blair, R. C., & Karniski, W. (1993). An alternative method for significance testing of waveform difference potentials. *Psychophysiology, 30*, 518–524.

Born, R. T., & Bradley, D. C. (2005). Structure and function of visual area MT. *Annual Review of Neuroscience, 28*, 157–189. http://dx.doi.org/10.1146/annurev.neuro.26.041002.131052.

Born, R. T., Groh, J. M., Zhao, R., & Lukasewycz, S. J. (2000). Segregation of object and background motion in visual area MT: Effects of microstimulation on eye movements. *Neuron, 26*(3), 725–734.

Born, R. T., & Tootell, R. B. (1992). Segregation of global and local motion processing in primate middle temporal visual area. *Nature, 357*(6378), 497–499. http://dx.doi.org/10.1038/357497a0.

Braddick, O. (1993). Segmentation versus integration in visual motion processing. *Trends in Neurosciences, 16*(7), 263–268.

Bremmer, F. (2005). Navigation in space – The role of the macaque ventral intraparietal area. *The Journal of Physiology, 566*(Pt 1), 29–35. http://dx.doi.org/10.1113/jphysiol.2005.082552.

Britten, K. H. (2008). Mechanisms of self-motion perception. *Annual Review of Neuroscience, 31*, 389–410. http://dx.doi.org/10.1146/annurev.neuro.29.051605.112953.

Britten, K. H., Shadlen, M. N., Newsome, W. T., & Movshon, J. A. (1992). The analysis of visual motion: A comparison of neuronal and psychophysical performance. *Journal of Neuroscience, 12*(12), 4745–4765.

Caplovitz, G. P., & Tse, P. U. (2007). V3A processes contour curvature as a trackable feature for the perception of rotational motion. *Cerebral Cortex, 17*(5), 1179–1189. http://dx.doi.org/10.1093/cercor/bhl029.

Cardin, V., Sherrington, R., Hemsworth, L., & Smith, A. T. (2012). Human V6: Functional characterisation and localisation. *PLoS ONE, 7*(10), e47685. http://dx.doi.org/10.1371/journal.pone.0047685.

Cardin, V., & Smith, A. T. (2010). Sensitivity of human visual and vestibular cortical regions to egomotion-compatible visual stimulation. *Cerebral Cortex, 20*(8), 1964–1973. http://dx.doi.org/10.1093/cercor/bhp268.

Cottereau, B. R., McKee, S. P., Ales, J. M., & Norcia, A. M. (2011). Disparity-tuned population responses from human visual cortex. *Journal of Neuroscience, 31*(3), 954–965.

Culham, J. C., Brandt, S. A., Cavanagh, P., Kanwisher, N. G., Dale, A. M., Tootell, R. B. H., et al. (2012). Cortical fMRI activation produced by attentive tracking of moving targets. *Journal of Neurophysiology*, 2657–2670.

De Jong, B. M., Shipp, S., Skidmore, B., Frackowiak, R. S. J., & Zeki, S. (1994). The cerebral activity related to the visual perception of forward motion in depth. *Brain, 117*(5), 1039–1054. http://dx.doi.org/10.1093/brain/117.5.1039.

Duffy, C. J., & Wurtz, R. H. (1991). Sensitivity of MST neurons to optic flow stimuli. I. A continuum of response selectivity to large-field stimuli. *Journal of Neurophysiology, 65*(6), 1329–1345.

Duffy, C. J., & Wurtz, R. H. (1997). Medial superior temporal area neurons respond to speed patterns in optic flow. *Journal of Neuroscience, 17*(8), 2839–2851.

Ferber, S., Humphrey, G. K., & Vilis, T. (2003). The lateral occipital complex subserves the perceptual persistence of motion-defined groupings. *Cerebral Cortex, 13*, 716–721.

Ferber, S., Humphrey, G. K., & Vilis, T. (2005). Segregation and persistence of form in the lateral occipital complex. *Neuropsychologia, 43*(1), 41–51. http://dx.doi.org/10.1016/j.neuropsychologia.2004.06.020.

Fesi, J. D., Yannes, M. P., Brinckmann, D. M., Ales, J. M., Norcia, A. M., & Gilmore, R. O. (2011). Distinct cortical responses to 2D figures defined by motion contrast. *Vision Research, 51*, 2110–2120.

Fischer, E., Bülthoff, H. H., Logothetis, N. K., & Bartels, A. (2012). Visual motion responses in the posterior cingulate sulcus: A comparison to V5/MT and MST. *Cerebral Cortex, 22*(4), 865–876.

Gibson, J. J. (1950). *The perception of the visual world*. Oxford, England: Houghton Mifflin.

Gilmore, R. O., Fesi, J. D., Thomas, A. L., & Hwang, K. R. (2011). *Connecting the dots: EEG responses at dot update rates reflect local motion and luminance modulation*. Washington, DC: The Society for Neuroscience.

Gilmore, R. O., Hou, C., Pettet, M. W., & Norcia, A. M. (2007). Development of cortical responses to optic flow. *Visual Neuroscience, 24*(6), 845–856. http://dx.doi.org/10.1017/S0952523807070769.

Gottlieb, J. P., Macavoy, M. G., & Bruce, C. J. (1994). Neural responses related to smooth-pursuit eye movements and their correspondence with electrically elicited smooth eye movements in the primate frontal eye field. *Journal of Neurophysiology, 72*, 1634–1653.

Grill-Spector, K., Kourtzi, Z., & Kanwisher, N. (2001). The lateral occipital complex and its role in object recognition. *Vision Research, 41*, 1409–1422.

Grill-Spector, K., Kushnir, T., Edelman, S., Avidan, G., Itzchak, Y., & Malach, R. (1999). Differential processing of objects under various viewing conditions in the human lateral occipital complex. *Neuron, 24*(1), 187–203.

Groppe, D. M., Urbach, T. P., & Kutas, M. (2011). Mass univariate analysis of event-related brain potentials/fields I: A critical tutorial review. *Psychophysiology, 48*(12), 1711–1725. http://dx.doi.org/10.1111/j.1469-8986.2011.01273.x.

Hadad, B.-S., Maurer, D., & Lewis, T. L. (2010). The development of contour interpolation: Evidence from subjective contours. *Journal of Experimental Child Psychology, 106*(2–3), 163–176. http://dx.doi.org/10.1016/j.jecp.2010.02.003.

Harvey, B. M., Braddick, O. J., & Cowey, A. (2010). Similar effects of repetitive transcranial magnetic stimulation of MT+ and a dorsomedial extrastriate site including V3a on pattern detection and position discrimination of rotating and radial motion patterns. *Journal of Vision, 10*, 1–15. http://dx.doi.org/10.1167/10.5.21.Introduction.

Hou, C., Gilmore, R. O., Pettet, M. W., & Norcia, A. M. (2009). Spatio-temporal tuning of coherent motion evoked responses in 4–6 month old infants and adults. *Vision Research, 49*(20), 2509–2517. http://dx.doi.org/10.1016/j.visres.2009.08.007.

Hubel, D. H., & Wiesel, T. N. (1968). Receptive fields and functional architecture of monkey striate cortex. *Journal of Physiology, 195*(1), 215–243.

Huk, A. C., Dougherty, R. F., & Heeger, D. J. (2002). Retinotopy and functional subdivision of human areas MT and MST. *Journal of Neuroscience, 22*(16), 7195–8205. http://dx.doi.org/20026661.

Kiorpes, L., & Movshon, J. A. (2004). Development of sensitivity to visual motion in macaque monkeys. *Visual Neuroscience, 21*(6), 851–859. http://dx.doi.org/10.1017/S0952523804216054.

Komatsu, H., & Wurtz, R. H. (1988). Relation of cortical areas MT and MST to pursuit eye movements. I: Localization and visual properties of neurons. *Journal of Neurophysiology, 60*(2), 580–603.

Kriegeskorte, N., Sorger, B., Naumer, M., Schwarzbach, J., van den Boogert, E., Hussy, W., et al. (2003). Human cortical object recognition from a visual motion flowfield. *Journal of Neuroscience, 23*(4), 1451–1463.

Krug, K., & Parker, A. J. (2011). Neurons in dorsal visual area V5/MT signal relative disparity. *Journal of Neuroscience, 31*(49), 17892–17904.

Lappe, M. (1998). A model of the combination of optic flow and extraretinal eye movement signals in primate extrastriate visual cortex. Neural model of self-motion from optic flow and extraretinal cues. *Neural Networks, 11*(3), 397–414.

Likova, L., & Tyler, C. W. (2008). Occipital network for figure/ground organization. *Experimental Brain Research, 189*(3), 257–267. http://dx.doi.org/10.1007/s00221-008-1417-6.

MacAvoy, M. G., Gottlieb, J. P., & Bruce, C. J. (1991). Smooth-pursuit eye movement representation in the primate frontal eye field. *Cerebral Cortex, 1*, 95–102.

Majaj, N., Carandini, M., & Movshon, J. (2007). Motion integration by neurons in macaque MT Is local, not global. *Journal of Neuroscience, 27*(2), 366–370.

Marcar, V. L., Xiao, D. K., Raiguel, S. E., Maes, H., & Orban, G. A. (1995). Processing of kinetically defined boundaries in the cortical motion area MT of the macaque monkey. *Journal of Neurophysiology, 74*(3), 1258–1270.

Marr, D., & Hildreth, E. (1980). Visual information processing: The structure and creation of visual representations. *Philosophical Transactions of the Royal Society of London, Series B: Biological sciences, 290*(1038), 199–218.

Mendola, J. D., Dale, A. M., Fischl, B., Liu, A. K., & Tootell, R. B. H. (1999). The representation of illusory and real contours in human cortical visual areas revealed by functional magnetic resonance imaging. *Journal of Neuroscience, 19*(19), 8560–8572.

Morrone, M. C., Tosetti, M., Montanaro, D., Fiorentini, A., Cioni, G., & Burr, D. C. (2000). A cortical area that responds specifically to optic flow, revealed by fMRI. *Nature Neuroscience, 3*(12), 1322–1328. http://dx.doi.org/10.1038/81860.

Movshon, J. A., & Newsome, W. T. (1996). Visual response properties of striate cortical neurons projecting to area MT in macaque monkeys. *Journal of Neuroscience, 16*(23), 7733–7741.

Naji, J. J., & Freeman, T. C. A. (2004). Perceiving depth order during pursuit eye movement. *Vision Research, 44*(26), 3025–3034. http://dx.doi.org/10.1016/j.visres.2004.07.007.

Nakamura, H., Kuroda, T., Wakita, M., Kusunoki, M., Kato, A., Mikami, A., et al. (2001). From three-dimensional space vision to prehensile hand movements: The lateral intraparietal area links the area V3a and the anterior intraparietal area in macaques. *Journal of Neuroscience, 21*(20), 8174–8187.

Nawrot, M. (2003a). Eye movements provide the extra-retinal signal required for the perception of depth from motion parallax. *Vision Research, 43*(14), 1553–1562. http://dx.doi.org/10.1016/S0042-6989(03)00144-5.

Nawrot, M. (2003b). Depth from motion parallax scales with eye movement gain. *Journal of Vision, 3*(11), 841–851. http://dx.doi.org/10.1167/3.11.17.

Nawrot, M., & Joyce, L. (2006). The pursuit theory of motion parallax. *Vision Research, 46*(28), 4709–4725. http://dx.doi.org/10.1016/j.visres.2006.07.006.

Nawrot, M., & Stroyan, K. (2009). The motion/pursuit law for visual depth perception from motion parallax. *Vision Research, 49*(15), 1969–1978. http://dx.doi.org/10.1016/j.visres.2009.05.008.

Nawrot, M., & Stroyan, K. (2012). Integration time for the perception of depth from motion parallax. *Vision Research, 59*, 64–71. http://dx.doi.org/10.1016/j.visres.2012.02.007.

Newsome, W., & Pare, E. (1988). A selective impairment of motion perception following lesions of the middle temporal visual area (MT). *Journal of Neuroscience, 8*(6), 2201–2211.

Newsome, W. T., Wurtz, R. H., & Komatsu, H. (1988). Relation of cortical areas MT and MST to pursuit eye movements. II. Differentiation of retinal from extraretinal inputs. *Journal of Neurophysiology, 60*(2), 604–620.

Ono, M. E., Rivest, J., & Ono, H. (1986). Depth perception as a function of motion parallax and absolute-distance information. *Journal of Experimental Psychology: Human Perception and Performance, 12*(3), 331–337.

Orban, G. A. (2011). The extraction of 3D shape in the visual system of human and nonhuman primates. *Annual Review of Neuroscience, 34*, 361–388. http://dx.doi.org/10.1146/annurev-neuro-061010-113819.

Pack, C. C., Gartland, A. J., & Born, R. T. (2004). Integration of contour and terminator signals in visual area MT of alert macaque. *Journal of Neuroscience, 24*(13), 3268–3280.

Perrone, J. A., & Krauzlis, R. J. (2008). Vector subtraction using visual and extraretinal motion signals: A new look at efference copy and corollary discharge theories. *Journal of Vision, 8*, 1–14. http://dx.doi.org/10.1167/8.14.24.Introduction.

Petit, L., Clark, V. P., Ingeholm, J., & Haxby, J. V. (1997). Dissociation of saccade-related and pursuit-related activation in human frontal eye fields as revealed by fMRI. *Journal of Neurophysiology, 77*, 3386–3390.

Peuskens, H., Claeys, K. G., Todd, J. T., Norman, J. F., Hecke, P. Van., & Orban, G. A. (2001). Attention to 3-D shape, 3-D motion, and texture in 3-D structure from motion displays. *Journal of Cognitive Neuroscience, 16*(4), 665–682.

Preston, T. J., Kourtzi, Z., & Welchman, A. E. (2009). Adaptive estimation of three-dimensional structure in the human brain. *Journal of Neuroscience, 29*(6), 1688–1698.

Preston, T. J., Li, S., Kourtzi, Z., & Welchman, A. E. (2008). Multivoxel pattern selectivity for perceptually relevant binocular disparities in the human brain. *Journal of Neuroscience, 28*(44), 11315–11327.

Regan, D., & Beverley, K. I. (1984). Figure-ground segregation by motion contrast and by luminance contrast. *Journal of the Optical Society of America A: Optics, Image Science, and Vision, 1*(5), 433–442.

Rivest, J., Ono, H., & Saida, S. (1989). The roles of convergence and apparent distance in depth constancy with motion parallax. *Perception and Psychophysics, 46*(5), 401–408.

Rizzolatti, G., Fogassi, L., & Gallese, V. (1997). Parietal cortex: From sight to action. *Current Opinion in Neurobiology, 7*(4), 562–567.

Rogers, B., & Graham, M. (1979). Motion parallax as an independent cue for depth-perception. *Perception, 8*(2), 125–134.

Stanley, D. A., & Rubin, N. (2003). FMRI activation in response to illusory contours and salient regions in the human lateral occipital complex. *Neuron, 37*(2), 323–331.

Stoner, G. R., & Albright, T. D. (1992). Motion coherency rules are form-cue invariant. *Vision Research, 32*(3), 465–475.

Tanaka, K., & Saito, H. (1989). Analysis of motion of the visual field by direction, expansion/contraction, and rotation cells clustered in the dorsal part of the medial superior temporal area of the macaque monkey. *Journal of Neurophysiology, 62*(3), 626–641.

Theys, T., Srivastava, S., Loon, J. Van, Goffin, J., & Janssen, P. (2012). Selectivity for three-dimensional contours and surfaces in the anterior intraparietal area. *Journal of Neurophysiology, 107*(3), 995–1008. http://dx.doi.org/10.1152/jn.00248.2011.

Thielscher, A., Kölle, M., Neumann, H., Spitzer, M., & Grön, G. (2008). Texture segmentation in human perception: A combined modeling and fMRI study. *Journal of Neuroscience, 151*(3), 730–736. http://dx.doi.org/10.1016/j.neuroscience.2007.11.040.

Thier, P., & Erickson, R. G. (1992). Responses of visual-tracking neurons from cortical area MST-I to visual, eye and head motion. *European Journal of Neuroscience, 4*(6), 539–553.

Tootell, R. B. H., Hadjikhani, N., Hall, E. K., Marrett, S., Vanduffel, W., Vaughan, J. T., et al. (1998). The retinotopy of visual spatial attention. *Neuron, 21*, 1409–1422.

Tsao, D. Y., Vanduffel, W., Sasaki, Y., Fize, D., Knutsen, T. A., Mandeville, J. B., et al. (2003). Stereopsis activates V3a and caudal intraparietal areas in macaques and humans. *Neuron, 39*, 555–568.

Victor, J. D., & Mast, J. (1991). A new statistic for steady-state evoked potentials. *Electroencephalography and Clinical Neurophysiology, 78*(5), 378–388.

Warren, W. H., & Hannon, D. J. (1988). Direction of self-motion is perceived from optical flow. *Nature, 336*(10), 162–163.

Wattam-Bell, J., Birtles, D., Hofsten, C. Von, Rosander, K., Anker, S., Atkinson, J., et al. (2010). Reorganization of global form and motion processing during human visual development. *Current Biology, 20*, 411–415. http://dx.doi.org/10.1016/j.cub.2009.12.020.

Weinstein, J. M., Gilmore, R. O., Shaikh, S. M., Kunselman, A. R., Trescher, W. V., Tashima, L. M., et al. (2011). Defective motion processing in children with cerebral visual impairment due to periventricular white matter damage. *Developmental Medicine & Child Neurology*. http://onlinelibrary.wiley.com/doi/10.1111/j.1469-8749.2010.03874.x/pdf.

Wexler, M., & van Boxtel, J. J. A. (2005). Depth perception by the active observer. *Trends in Cognitive Sciences, 9*(9), 431–438. http://dx.doi.org/10.1016/j.tics.2005.06.018.